

Electron Exchange in Conformationally Restricted Donor–Spacer–Acceptor Dyads: Angle Dependence and Involvement of Upper-Lying Excited States

Andrew C. Benniston, Anthony Harriman,* Peiyi Li, Pritesh V. Patel, and Craig A. Sams^[a]

Abstract: The rate constant for triplet energy transfer (k_{TET}) has been measured in fluid solution for a series of mixed-metal Ru–Os bis(2,2':6',2''-terpyridine) complexes built around a tethered biphenyl-based spacer group. The length of the tether controls the central torsion angle for the spacer, which can be varied systematically from 37 to 130°. At low temperature, but still in fluid solution, the spacer adopts the lowest-energy conformation and k_{TET} shows a clear correlation with the torsion angle. A similar relationship holds for the inverse quantum yield for emission from the Ru–terpy donor. Triplet energy transfer is more

strongly activated at higher temperature and the kinetic data require analysis in terms of two separate processes. The more weakly activated step involves electron exchange from the first-excited triplet state on the Ru–terpy donor and the size of the activation barrier matches well with that calculated from spectroscopic properties. The pre-exponential factor derived for this process correlates remarkably well

with the torsion angle and there is a large disparity in electronic coupling through π and σ orbitals on the spacer. The more strongly activated step is attributed to electron exchange from an upper-lying triplet state localized on the Ru–terpy donor. Here, the pre-exponential factor is larger but shows the same dependence on the geometry of the spacer. Strangely, the difference in coupling through π and σ orbitals is much less pronounced. Despite internal flexibility around the spacer, k_{TET} shows a marked dependence on the torsion angle computed for the lowest-energy conformation.

Keywords: donor–acceptor systems • energy transfer • laser chemistry • time-resolved spectroscopy • triplet states

Introduction

It is known that the strength of electronic coupling between remote donor–acceptor pairs is sensitive to the length,^[1] composition,^[2] and conformation^[3] of the connecting spacer group in donor–spacer–acceptor (D–Sp–A) molecular dyads. Additional modulation of the coupling element arises from variation of the mutual orientations^[4] and of the energy gap^[5] between donor and spacer orbitals. Numerous theoretical studies have addressed the issue of how the magnitude of the coupling matrix element (V_{DA}) varies with the geometry of the spacer unit.^[6] This work has been complemented by experimental studies with covalently linked D–Sp–A

dyads,^[7] but it has proved difficult to produce systematic series of dyads that differ only in the geometry of the spacer. For example, varying the torsion angle between two interconnected phenyl rings using bulky substituents at the 2- or 2,2'-position(s) also affects the electronic properties of the spacer group. Even so, astonishing success has been realized with single-molecule conductance measurements with the spacer unit suspended between metallic electrodes.^[8] Here it has been shown^[9] that there is a 20-fold variation in conductance between planar and orthogonal phenylene rings and that the variation in conductance shows a \cos^2 dependence on the dihedral angle at the biphenyl connection. Furthermore, this work confirms that electron transfer through the π -orbitals is much more effective than through the corresponding σ orbitals.^[9]

Considerable information has accrued regarding the electron-transfer dynamics for rigid D–Sp–A dyads, but conformational heterogeneity introduces severe problems when interpreting such data for flexible or semiflexible analogues.^[10] One solution to this problem involves embedding the dyad in a glassy matrix^[11] or viscous solvent.^[12] A more demand-

[a] Dr. A. C. Benniston, Prof. A. Harriman, Dr. P. Li, Dr. P. V. Patel, Dr. C. A. Sams
Molecular Photonics Laboratory
School of Natural Sciences, University of Newcastle
Newcastle upon Tyne, NE1 7RU (UK)
Fax: (44) 191-222-8660
E-mail: Anthony.harriman@ncl.ac.uk

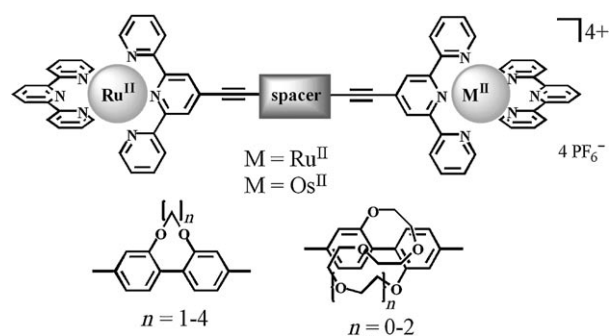
ing approach uses time-resolved infrared spectroscopy^[13] to monitor the dynamics of any conformational exchange that competes with light-induced electron transfer. In the following work, we investigate if the internal flexibility of the spacer, this having been confirmed by molecular dynamics simulations (MDS),^[14] affects the rate of electron exchange in semi-rigid D-Sp-A dyads. The spacer is composed of a strapped 2,2'-dialkoxybiphenyl unit in which the length of the strap controls the torsion angle between the two phenyl rings.^[14] Although these straps collapse into the lowest-energy conformation in a low temperature glass, thereby facilitating a correlation between torsion angle and rate of electron exchange,^[15] a wider range of torsion angles is to be expected in fluid solution. The main objective of this study is to establish if the global rate constant for electron exchange in such dyads still remembers the mean torsion angle pertaining to the lowest-energy conformer. A critical aspect of the work, especially with respect to designing electronic switches, is to assess the relative importance of electron tunnelling through σ and π bonds. This can be done by comparing the magnitude of V_{DA} for parallel and perpendicular geometries of the biphenyl-based spacer.

We have previously reported electron exchange in these same molecules at low temperature^[15] at which conformational motion is severely retarded. Results similar to those reported for single-molecule conductance were noted,^[9] with an 80-fold variation in the rates for planar and orthogonal geometries. Also, the rates adhered to a crude \cos^2 relationship with the central dihedral angle. We now examine what happens in fluid solution at ambient temperature and emphasize any differences from the behaviour found in a glassy matrix. It should also be noted that electron exchange has been described^[16] in a related trinuclear complex built from similar modules.

Results and Discussion

The binuclear complexes, and their abbreviations, used in this study are described in Scheme 1. The symmetrical Ru–Ru complexes are used as reference compounds with which to examine the rates of intramolecular electron exchange in the Ru–Os mixed-metal complexes. Synthesis, purification and full characterization are reported elsewhere,^[14] as is a description of the MDS studies. The strap length imposes a preferred torsion angle (φ) for the biphenyl spacer unit and this property varies from 37° for the shortest strap to 130° for the longest analogue (Table 1). Because of steric constraints, this strategy does not permit isolation of the planar geometry, but the number of compounds is increased on binding simple cations to the central void inherent to the crown ether strap. Details of the photophysical properties of the binuclear Ru–Ru complexes are available in the literature,^[17] as is a separate study of cation binding.^[18]

The absorption spectra of the various mixed-metal complexes are essentially superimposable and the characteristic



Scheme 1. Molecular formulae for the various binuclear complexes investigated here. The abbreviations use R and O, respectively, to refer to ruthenium(II) and osmium(II) cations, while C refers to a hydrocarbon-based strap and CE to a corresponding crown ether strap. The numeral included in the abbreviation refers to the number of carbon atoms in the hydrocarbon strap or the number of oxygen atoms in the crown ether.

Table 1. Properties of the binuclear complexes in fluid solution at room temperature.

	φ [°] ^[a]	Φ_{LUM} ^[b]	τ_{LUM} [ns] ^[b]	τ_{Ru} [ns] ^[c]
RC1O	37	0.0015	170	21
RC2O	55	0.0025	165	24
RC3O	67	0.0025	170	22
RC4O	94	0.0020	150	25
RCE4O	122	0.0025	150	24
RCE5O	125	0.0020	155	26
RCE6O	130	0.0030	150	26

[a] Obtained for the lowest-energy conformation from computational chemistry studies. [b] Refers to emission from the Os–terpy unit. [c] Refers to the corresponding Ru–Ru binuclear complex.

features of a metal–poly(pyridine) complex are easily recognized. For the mixed-metal complexes, there is a pronounced spin-forbidden transition at wavelengths longer than 600 nm that can be used for selective excitation into the Os–terpy unit (terpy = 2,2':6',2''-terpyridine).^[19] The spin-allowed, metal-to-ligand, charge-transfer (MLCT) transitions on the two metal complexes appear as a single transition centered at about 500 nm, while the spacer unit absorbs at around 300 nm (Figure 1). In deoxygenated acetonitrile at ambient temperature, emission can be seen from the mixed-metal complexes. This luminescence band is centered at

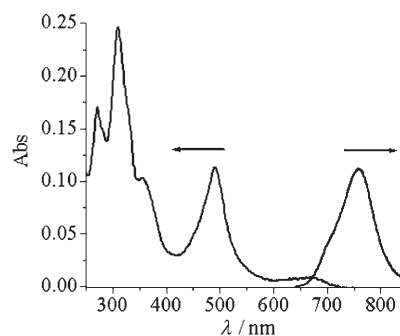


Figure 1. Absorption and emission spectra recorded for RC3O in acetonitrile at room temperature. The excitation wavelength was 460 nm.

around 760 nm, but shows a pronounced shoulder at about 695 nm (Figure 1). Comparison with appropriate reference compounds,^[19] including the corresponding Ru–Ru complexes,^[17] shows that this emission arises from the Os–terpy unit. The spectral profile is independent of excitation wavelength and there is good agreement between excitation and absorption spectra across the entire region. The emission decays with first-order kinetics with a lifetime (τ_{LUM}) in the order of 160 ± 15 ns at 295 K (Table 1). Under the same conditions, the emission quantum yield (Φ_{LUM}) is around 0.0025 ± 0.0010 and is insensitive to the strap length (Table 1). It is tempting to assign the shoulder seen at 695 nm to emission from the Ru–terpy unit, but this is most unlikely. Thus, the same profile is seen when only the Os–terpy unit is excited and is still evident in the mononuclear complex bearing an ethyne substituent. This emission band, for which the intensity increases with increasing temperature, is safely assigned to hot emission from the fourth MLCT triplet state localized on the Os–terpy unit.^[19,20] It is coincidence that the peak is in a position expected for the Ru–terpy complex.

Nanosecond laser flash photolysis studies made for the Ru–Os binuclear complexes in deoxygenated acetonitrile at room temperature are also characteristic of the Os–terpy unit (Figure 2). The differential absorption spectrum shows

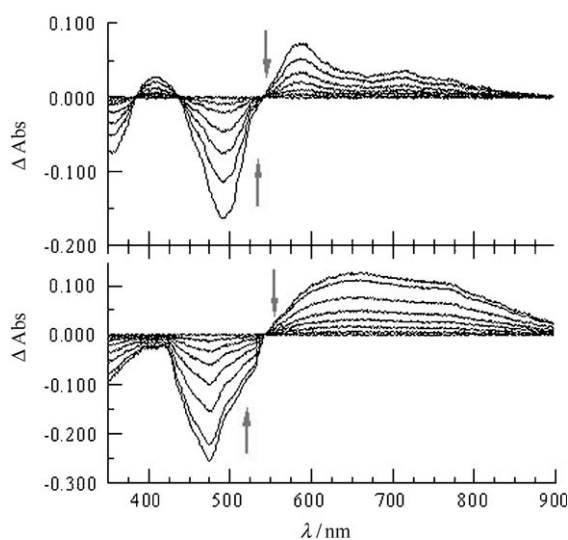


Figure 2. Transient differential absorption spectra recorded after laser excitation ($\lambda = 480$ nm; FWHM = 4 ns) of RC3O (top) and RC3R (bottom) in deoxygenated acetonitrile at room temperature. Spectra were recorded at different times after the excitation pulse.

bleaching of the MLCT transition at 500 nm and weak absorption at lower and higher energies. The spectrum is independent of excitation wavelength, on these timescales, and insensitive to changes in strap length. Lifetimes recorded for the triplet states are very similar to those derived by time-resolved emission spectroscopy. For the Ru–Ru binuclear complexes, the differential transient absorption spectra differ from those described above (Figure 2), while the life-

times (τ_{Ru}) are on the order of 25 ± 5 ns at room temperature (Table 1). The peak of the bleaching signal is blue shifted to about 485 nm—this is an important marker by which to monitor intramolecular triplet-energy transfer—while there is more pronounced absorption in the far-red region. Consequently, we can conclude that efficient energy transfer occurs from Ru–terpy to Os–terpy at ambient temperature in fluid solution. This behaviour is similar to that found in a glassy matrix,^[15] but the dynamics are faster in solution.

On cooling a solution of the Ru–Os mixed-metal complexes in butyronitrile, and using an excitation wavelength of 480 nm at which the Ru–terpy unit absorbs 65% of incident photons, the total emission intensity increases progressively. In addition, a new emission band becomes apparent at higher energy and is centered at about 675 nm (Figure 3).

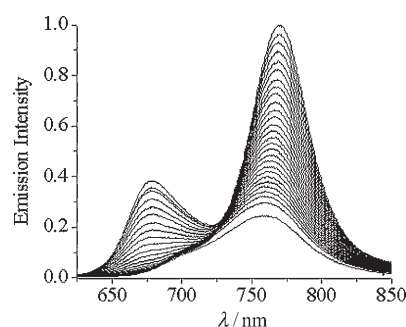


Figure 3. Effect of decreasing the temperature on the emission spectrum recorded for RC3O in deoxygenated butyronitrile. The excitation wavelength was 480 nm. Spectra were recorded at 10 K intervals from 290 to 160 K.

This latter emission can be assigned^[17] to the Ru–terpy unit by comparison to the corresponding Ru–Ru binuclear complexes. The relative intensity of this emission is always much less than that of the Os–terpy unit, despite the more favourable absorption profile of the Ru–terpy unit. This situation can be well explained in terms of activated triplet-energy transfer along the molecular axis.^[16] As such, luminescence from the Ru–terpy unit becomes more favourable as the temperature is lowered. It should also be noted that the photophysical properties of the Ru–Ru binuclear complexes^[17] are strongly dependent on temperature, because of thermal population of a high-lying, metal-centered triplet state that is coupled to the ground state. Thus, decreasing the temperature serves to both slow down triplet-energy transfer and raise the emission probability for the Ru–terpy donor. The net result is a steady increase in emission from the Ru–terpy unit as the temperature decreases.

To confirm that the new emission band is indeed due to the Ru–terpy unit, a detailed spectral deconvolution was made for low-temperature spectra for which the overall intensity is relatively high (Figure 4). Under these conditions, the observed spectrum can be split into two series, each composed of three bands. The low-energy series corresponds to emission from the Os–terpy unit^[19] and has a 0,0-transition at 13030 cm^{-1} . The series is composed of low

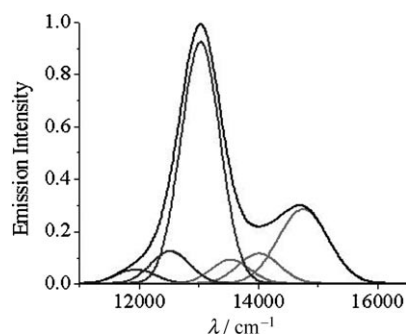


Figure 4. Deconvolution of the emission spectrum recorded for RC3O in deoxygenated butyronitrile at 190 K into components belonging to the individual terminals. The spectra corresponding to Ru–terpy are shown in light grey and those for Os–terpy are shown in dark grey.

($h\nu_L=515\text{ cm}^{-1}$) and medium ($h\nu_M=1,095\text{ cm}^{-1}$) frequency vibrational modes coupled to the decay process. These values are fully consistent with emission from an Os–terpy unit bearing a single ethyne substituent. Likewise, the high-energy series, for which the 0,0-transition is located at 14750 cm^{-1} , can be attributed to the Ru–terpy unit by reference to earlier work^[19,21] and by comparison to the Ru–Ru binuclear complexes.^[17] Here, the vibrational progression includes low ($h\nu_L=750\text{ cm}^{-1}$) and medium ($h\nu_M=1,225\text{ cm}^{-1}$) frequency modes. It should be noted that the small but significant increase in emission yield found for the Os–terpy unit is entirely consistent with previous work carried out with ethynylated Os–terpy derivatives.^[19] Here, the rate constant for nonradiative decay of the Os–terpy triplet state decreased a factor of about three on cooling from 290 K to 160 K. The difference in 0,0-transitions can be used to give an estimate of the energy gap ($\Delta E_{\text{TT}}=1,720\text{ cm}^{-1}$) between donor and acceptor triplets. Furthermore, analysis of the emission band shapes as a function of temperature allows calculation of the total reorganization energy accompanying triplet-energy transfer (λ_{TT}) as being 1000 cm^{-1} .

By using this spectral deconvolution procedure, the quantum yields for emission from the Ru–terpy unit at 170 K were determined by reference to the Ru–Ru binuclear complexes and allowing for the percentage (i.e., 65 %) of light absorbed by this chromophore. The derived values (Φ_{LUM}) are collected in Table 2. At this temperature, butyronitrile is

Table 2. Properties of the binuclear complexes in butyronitrile at 170 K.

	$10^5 \Phi_{\text{LUM}}^{[a]}$	$\tau_{\text{LUM}} [\text{ns}]^{[a]}$	$\tau_{\text{Ru}} [\text{ns}]^{[b]}$	$k_{\text{TET}} [10^8 \text{ s}^{-1}]$
RC1O	<3	2.1	415	4.6
RC2O	8	6.2	320	1.6
RC3O	23	19.8	390	0.48
RC4O	140	140	1280	0.06
RCE4O	20	18.2	360	0.52
RCE5O	13	11.3	460	0.86
RCE5O/Na ⁺	160	145	1470	0.06
RCE6O	5	4.7	360	2.1
RCE6O/Na ⁺	15	13.2	1205	0.75
RCE6O/K ⁺	46	40.4	1495	0.24

[a] Refers to emission from the Ru–terpy unit. [b] Refers to the corresponding Ru–Ru binuclear complex.

fluid, but [presumably] highly viscous. The quantum yields are low, but there is a clear correlation with the length of the strap, leading to a 50-fold variation throughout the series. Moreover, the emission lifetimes measured at this temperature (τ_{Ru}), these being much more accurate than the Φ_{LUM} values, show a definite trend as the central dihedral angle changes (Table 2). We can calculate the rate constant (k_{TET}) for triplet-energy transfer by comparing lifetimes measured for appropriate pairs of Ru–Os and Ru–Ru complexes (Table 2), restricting attention to the Ru–terpy unit. At 170 K, it can be seen that k_{TET} correlates nicely with the central torsion angle, with a minimum at 90° and a maximum at 0° . At this temperature, it is reasonable to suppose that the strap adopts the lowest-energy conformation and the behaviour found at 170 K tends to confirm the situation already known to exist in the glassy matrix in which k_{TET} is highly dependent on the dihedral angle.^[15] The large uncertainty associated with the measured Φ_{LUM} values and the limited information that be extracted from a single temperature^[16] preclude detailed analysis of these results in terms of their exact correlation with φ .

Emission from the Ru–terpy donor is too weak for similar measurements to be made at ambient temperature and there is the additional problem that the inherent triplet lifetime of the donor, measured for the Ru–Ru binuclear complexes,^[17] is much shorter under these conditions (Table 1). As such, triplet-energy transfer has to compete with fast nonradiative decay of the donor triplet. The required rate constants were derived by laser flash photolysis studies carried out as a function of temperature and with 50 ps temporal resolution. From the transient spectra shown in Figure 2, it appears that the Ru–terpy triplet can be monitored with reasonable selectivity at approximately 750 and 450 nm. This situation is confirmed by the studies carried out for RC3O, for which the spectral records evolve steadily over a few nanoseconds following laser excitation at 480 nm (Figure 5). The final spectrum, recorded at 10 ns, agrees well with that found during the ns laser flash photolysis studies and assigned to the Os–terpy triplet, but there are clear kinetic processes apparent on shorter time scales (Figure 6).

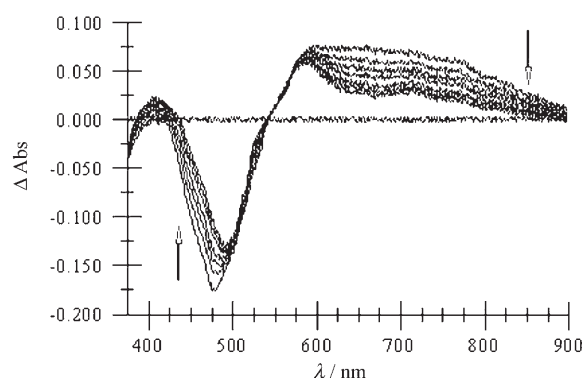


Figure 5. Transient differential absorption spectra recorded after laser excitation of RC3O in deoxygenated butyronitrile at room temperature. Spectra were recorded at delay times of 0, 0.5, 1.0, 1.5, 2, 3, 4, and 6 ns.

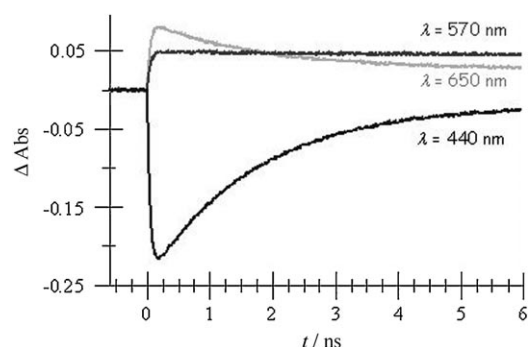


Figure 6. Kinetic decay traces recorded after laser excitation of RC3O in deoxygenated butyronitrile. Individual traces were recorded at 440, 570, and 650 nm.

On the basis of a global fit to the sum of exponentials, the lifetime for the Ru-terpy unit in RC3O is derived to be 1.7 ± 0.2 ns at 295 K. The corresponding Os-terpy triplet does not decay on this timescale. Comparing the lifetime found for the Ru-terpy unit in RC3O with that in RC3R ($\tau_T = 22 \pm 3$ ns), we find that $k_{TET} = 5.3 \times 10^8 \text{ s}^{-1}$ under these conditions. Repeating this rather tedious procedure from 295 to 160 K allows determination of the temperature dependence for triplet-energy transfer in fluid butyronitrile.

The results of these temperature-dependent studies can be expressed in the form of an Arrhenius-type plot (Figure 7). It is seen that, for each system, k_{TET} tends towards a weakly activated process at low temperature, but the rate is more strongly activated at higher temperature. Comparable behaviour was noted previously for the trinuclear complex.^[16] Before attempting to analyze these data it is worth stressing that triplet-energy transfer is essentially quantitative in all cases and that no other competing process is apparent from the flash photolysis records. That is to say, no intermediate species could be detected. Furthermore, we consider that triplet-energy transfer occurs exclusively by way of through-bond electron exchange, which can be described in terms of simultaneous transfer of an electron and

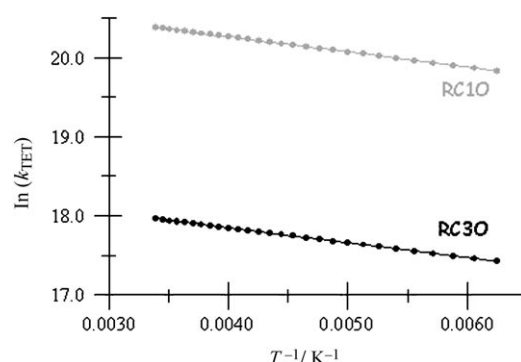


Figure 7. Arrhenius-type plots made for triplet-energy transfer in RC10 (grey) and RC3O (black) dissolved in deoxygenated butyronitrile. The solid lines drawn through the data points are the best least-squares fits to two activated processes.

a positive hole.^[22] This allows the reaction to be considered in terms of Marcus theory.^[23]

As mentioned above, analysis of the temperature-dependent kinetic data (Figure 7) demands two activated processes with disparate activation parameters. Assuming that both steps are controlled by long-range electron exchange, data analysis can be attempted along the lines set by Equation (1). Here, the two activated processes are assigned pre-exponential factors of A and B , respectively, and each has an associated free-energy of activation, denoted as E_A and E_B respectively. The only constraints imposed on the system are that $A \ll B$ and $E_A \ll E_B$. As such, the lower-temperature region provides information about A , whereas process B dominates in the high temperature limit. Focussing firstly on the low-temperature region, it appears that the activation barrier E_A is independent of strap length and has an averaged value of about 130 cm^{-1} (Table 3). This is a relatively

Table 3. Values for the pre-exponential factors and activation barriers derived from the temperature-dependence studies made in butyronitrile.^[a]

	A [$10^7 \text{ s}^{-1} \text{ K}^{1/2}$]	E_A [cm^{-1}]	B [$10^{10} \text{ s}^{-1} \text{ K}^{1/2}$]	E_B [cm^{-1}]
RC1O	137	135	30	1150
RC2O	38	120	18	1090
RC3O	12	132	11	1130
RC4O	0.95	133	4.6	1140
RCE4O	14	128	5.3	1120
RCE5O	25	136	8.5	1130
RCE5O/Na ⁺	1.3	124	2.6	1160
RCE6O	59	130	15	1120
RCE6O/Na ⁺	21	132	6.1	1110
RCE6O/K ⁺	6.1	126	5.0	1160

[a] Refer to Equations (1)–(4).

small barrier, showing the process to be weakly activated. It is well explained in terms of Equation (2), with $\Delta E_{TT} = 1720 \text{ cm}^{-1}$, $\lambda_{TT} = 1000 \text{ cm}^{-1}$ and $n=0$. This last term refers to the number of medium-frequency vibrational modes that contribute to the activation energy.^[24] The derived values of A vary significantly throughout the series and it is clear that there exists a precise relationship between A and the central torsion angle, φ (Table 3). Indeed, A is at a minimum when φ approaches 90° and at a maximum for the coplanar geometry of the spacer. To take due account of this angle dependence, and allowing for the absence of quantum mechanical effects (i.e., $n=0$), it is possible to express A in terms of Equation (3). Here, V_σ and V_π refer to the electronic coupling matrix elements for electron tunnelling through σ and π orbitals, respectively, and χ is as described by Equation (4), with S being the Huang-Rhys factor.^[25] On the basis of these equations, we might expect that A should scale according to $\cos^4 \varphi$.

$$k_{TT} \sqrt{T} = A e^{-\frac{E_A}{k_B T}} + B e^{-\frac{E_B}{k_B T}} \quad (1)$$

$$E_A = \frac{(\lambda_{TT} + nh\omega_M - \Delta E_{TT})^2}{4\lambda_{TT}} \quad (2)$$

$$A = \chi(V_o + V_\pi \cos^2 \phi)^2 \quad (3)$$

$$\chi = \frac{2\pi}{\hbar\sqrt{4\pi k_B \lambda_{TT}}} \sum_{n=0}^{\infty} e^{-S} \left(\frac{S^n}{n!} \right) \quad (4)$$

The experimental results fully support this hypothesis (Figure 8). By extrapolation, it appears that A varies by a factor of almost 350-fold for parallel and perpendicular geo-

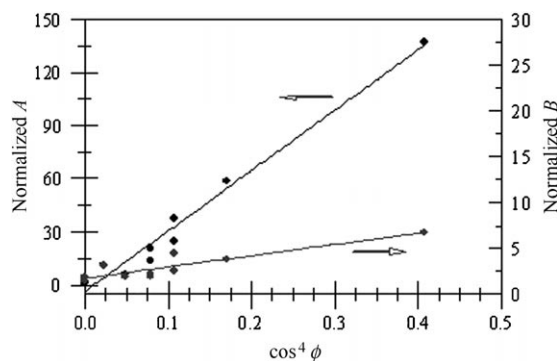


Figure 8. Relationship between the normalized pre-exponential factors A and B (units: $\text{s}^{-1}\text{K}^{1/2}$) and the central torsion angle of the bridging biphenyl unit.

metries of the spacer unit. Electron exchange across the coplanar geometry is predicted to occur with a pre-exponential factor of about $3.4 \times 10^9 \text{ s}^{-1}\text{K}^{1/2}$. Furthermore, values for V_o and V_π of 0.027 and 0.52 cm^{-1} , respectively, can be derived from these limits. This relative ordering compares well with the factor of approximately 20 obtained from single-molecule conductance studies made with substituted biphenyl derivatives.^[9] The difference is significantly more pronounced than that found previously for hole transfer through related systems, for which the coupling element increased by a factor less than twofold on moving from orthogonal to coplanar geometries.^[26] This latter finding might be suggestive of the possibility that different electronic processes have disparate sensitivities towards such angular effects. If correct, this would be a most important finding, because it would provide the opportunity to employ such angular constraints as a means by which to discriminate between rates of forward and reverse electron transfer in molecular dyads. All indications point to process A being associated with long-range electron exchange from the lowest excited triplet state of the Ru-terpy donor to the corresponding triplet state localized on the Os-terpy acceptor. It is remarkable that the integrity of the torsion-angle dependence is maintained for this process, given the inherent flexibility of the spacer and the fact that the surrounding medium is fluid.

Attention can now be turned to the more strongly activated process associated with B for which the activation barrier (E_B) appears to be independent of strap length and tends to-

wards an average value of 1130 cm^{-1} . The derived values for B greatly exceed those found for A (Table 3), but show a similar dependence on strap length (Figure 8). In this case, the limiting pre-exponential factor for the co-planar geometry is extrapolated to be $6.4 \times 10^{11} \text{ s}^{-1}\text{K}^{1/2}$ and is some 15-fold higher than that found for the orthogonal geometry. This means that the sensitivity towards the angle dependence is much less pronounced than for process associated with A . Since B exceeds $3.4 \times 10^9 \text{ s}^{-1}\text{K}^{1/2}$ it cannot refer to long-range electron exchange across the co-planar geometry. In turn, E_B cannot be associated with internal twisting of the spacer to reach a co-planar geometry, because this would require B to be independent of strap length and for E_B to vary with torsion angle. Neither of these features is apparent in the experimental results. Likewise there is no reason to suppose that the spacer has a relatively low-lying π, π^* triplet state that can be accessed from the donor triplet at elevated temperatures.^[27]

Although the energy of the π, π^* triplet is unknown, there is no indication for coupling between this state and the lowest-energy MLCT triplet state localized on the Ru-terpy donor. Such interaction should lead to a prolongation of the lifetime of the MLCT triplet and it is clear that this is not the case for the Ru–Ru binuclear complexes. An alternative explanation that fits all the observations, and takes due account of earlier work made with several ethynylated Ru-terpy derivatives,^[17,19] is that the process associated with B involves thermal population of the so-called fourth MLCT triplet state localized on the donor. This species is believed to reside about 580 cm^{-1} above the lowest-energy triplet ensemble^[17,19] and has been detected by luminescence spectroscopy for the Ru–Ru binuclear complexes. Our kinetic results can be [tentatively] interpreted in terms of this upper-lying triplet state acting as a donor for long-distance triplet-energy transfer.

To do so, we can consider the overall situation in terms of the potential-energy-level diagram presented as Figure 9. Here, triplet-energy transfer from the lowest-energy MLCT

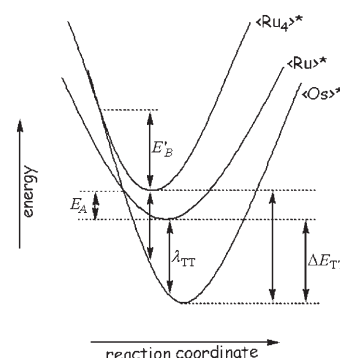


Figure 9. Potential-energy-level diagram proposed to explain triplet-energy transfer in the mixed-metal binuclear complexes. The symbols $\langle \text{Os} \rangle^*$, $\langle \text{Ru} \rangle^*$, and $\langle \text{Ru}_4 \rangle^*$ refer to the lowest-energy MLCT triplet states localized on Os-terpy and Os-terpy and the so-called fourth MLCT triplet on Ru-terpy, respectively. The activation energies, energy gaps, and total reorganization energies are marked. Note, E'_B refers to the electron exchange contribution to E_B .

triplet state on the Ru–terpy donor is slightly inverted and the donor–acceptor pair is weakly coupled. The fourth MLCT triplet localized on the Ru–terpy donor resides some 580 cm^{-1} above the lower-energy MLCT triplet such that ΔE_{TT} increases to 2300 cm^{-1} . This pushes the consequent triplet–energy transfer step deeper into the inverted region—a detailed analysis^[17,19] of the emission spectral profile shows that λ_{T} for the fourth MLCT triplet is decreased to 350 cm^{-1} , compared to 510 cm^{-1} for the lowest-energy MLCT triplet. Thus, the activation barrier for this process is calculated from Equation (2) ($n=0$) to be about 635 cm^{-1} . The average value for E_{B} ($=1130\text{ cm}^{-1}$) obtained by experiment compares extremely well with the sum ($=1215\text{ cm}^{-1}$) of the energy gap between the two MLCT triplets and the calculated activation barrier. As such, we can attribute the more strongly activated process to a combination of thermal population of the upper-lying triplet and the subsequent activation energy for electron exchange. Within this model, and with $\lambda_{\text{TT}}=840\text{ cm}^{-1}$, V_{σ} and V_{π} values of 1.7 and 5.3 cm^{-1} , respectively, are calculated from the limits set by Figure 8.

It is notable that electronic coupling between the reactants is markedly different for the two MLCT triplet states. Earlier work has shown that the fourth MLCT possesses somewhat more “singlet” character^[28] than the lower-lying ensemble and couples more strongly to the metal-centered triplet state. What is especially significant is the observation that V_{σ} is greatly increased for the uppermost MLCT triplet. Indeed, whereas there is a 12-fold increase in V_{π} on moving to the upper-lying state, the increase in V_{σ} is 55-fold. It seems unlikely that such a large increase can be explained in terms of the smaller energy gap between the donor and spacer.^[29] A proper explanation of this effect, however, must wait until more datasets have been acquired.

Conclusion

In pursuing the notion of an angle dependence in fluid solution we have encountered several important points: Firstly, the sensitivity of k_{TET} towards the central torsion angle imposed on the spacer is preserved in solution and is not dampened out by fluctuations. In effect, it seems likely that internal motion around the connecting bond is accompanied by a small activation energy that is encompassed in the global E_{A} term. The full effect of viscosity is unlikely to be exerted, since the geometry change is modest and the molecule might well reside in a cavity inside the solvent structure, even at low temperature. This opens up the possibility to design electronic switches that operate at the molecular level by inducing a large-scale change in the conformation of a biphenyl-based spacer unit. As such, the next phase of the operation is to devise a suitable switching mechanism.

It has also been shown that intramolecular triplet–energy transfer can take place from the so-called^[30] fourth MLCT triplet state associated with the Ru–terpy donor. Recently, it was established that this latter triplet state is prominent for

ethynylated terpy derivatives and some of its spectroscopic properties have been determined.^[17,19] It is believed to possess more “singlet-like” character than the lowest-energy MLCT triplet state and it is known to couple strongly to the metal-centered triplet localized on the Ru–terpy unit. The real significance of this finding is that the fourth MLCT triplet has a much higher electronic coupling matrix element for electron exchange than is available to the normal MLCT triplet. This is especially so for coupling through the sigma orbital and consequently k_{TET} displays non-Arrhenius behaviour. The possibility that the sensitivity to the angular effect decreases with increasing V_{DA} is intriguing, although we have only three datasets, and might offer a chance to control electron-transfer rates. This realization has special relevance to the stabilization of charge-separated states against fast charge recombination.

Finally, it should be noted that the tethered spacers are inherently chiral and, in certain cases, it should be possible to resolve the mixture of atropisomers. This would enable a systematic evaluation of how the rates of electron transfer depend on the handedness of the spacer,^[31] a feature of great interest in biological processes. Recent work with macroscopic electrodes twisted into helical wires has concluded that the electrical resistance of the conductor depends on its handedness. We now have the opportunity to test this hypothesis at the molecular level.

Experimental Section

Detailed synthetic procedures to obtain the title compounds have been described previously.^[14] The compounds were purified by extensive silica gel chromatography ($\text{CH}_3\text{CN}/\text{H}_2\text{O}/\text{KNO}_3(\text{aq})$) and identified by a number of analytical techniques including electrospray and MALDI mass spectrometry, $^1\text{H NMR}$ spectroscopy, and elemental analysis. Prior to making the spectroscopic studies, each complex was passed down a preparative thin-layer chromatography (tlc) plate using spectroscopic grade solvents to avoid the introduction of luminescent impurities. The binding of cations (Li^+ , Na^+ , K^+) in the crown ether cavities for RCE5O and RCE6O (for a definition of the abbreviations see legend of Scheme 1) was studied by using simple biphenyl-based polyether analogues. To summarize the findings, the ES mass spectral records confirmed a metal:ligand ratio of 1:1 across the whole cation series, with no sign of higher order assemblies. The association constants for the ligands towards the various cations in acetonitrile, as measured by fluorescence quenching experiments,^[18] were in the order of $3\text{--}7500\text{ m}^{-1}$. Quantum chemical calculations were used to obtain dihedral angles and molecular dynamics simulations provided the variation in angle around the mean value.^[14]

The instrumentation used for the spectroscopic studies has been described before.^[17,19] The sample was dissolved in butyronitrile and thoroughly deoxygenated. The temperature was controlled with an Oxford Instruments Optisat DN cryostat and emission studies were made with a Jobin–Yvon Fluorolog tau-3 spectrophotometer. Time-resolved emission studies were made by time-correlated, single-photon counting methods. Laser flash photolysis studies were made with a series of instruments, according to the time resolution required for that particular measurement. All studies were made by comparison of the Ru–Os and Ru–Ru complexes under identical conditions.

Acknowledgement

We thank the EPSRC (GR/R23305/01) and Newcastle University for financial support of this work.

- [1] a) W. B. Davis, M. A. Ratner, M. R. Wasielewski, *Chem. Phys.* **2002**, *281*, 333–346; b) S. F. Nelsen, M. D. Newton, *J. Phys. Chem. A* **2000**, *104*, 10023–10031.
- [2] M. J. Shephard, M. N. Paddon-Row, K. D. Jordan, *Chem. Phys.* **1993**, *176*, 289–304.
- [3] a) V. Mujica, A. Nitzan, Y. Mao, W. Davis, M. Kemp, A. Roitberg, M. A. Ratner, *Adv. Chem. Phys.* **1999**, *107*, 403–429; b) A. C. Benniston, A. Harriman, *Chem. Soc. Rev.* **2006**, *35*, 169–179.
- [4] a) S. H. Ke, H. U. Baranger, W. T. Yang, *J. Am. Chem. Soc.* **2004**, *126*, 15897–15904; b) L. Karki, J. T. Hupp, *J. Am. Chem. Soc.* **1997**, *119*, 4070–4073; c) V. S. Y. Lin, M. J. Therien, *Chem. Eur. J.* **1995**, *1*, 645–651.
- [5] a) J. Wiberg, L. J. Guo, K. Pettersson, D. Nilsson, T. Ljungdahl, J. Martensson, B. Albinsson, *J. Am. Chem. Soc.* **2007**, *129*, 155–163; b) L. A. Curtiss, C. A. Naleway, J. R. Miller, *Chem. Phys.* **1993**, *176*, 387–405; c) C. X. Liang, M. D. Newton, *J. Phys. Chem.* **1993**, *97*, 3199–3211.
- [6] a) M. D. Newton, *Int. J. Quantum Chem.* **2000**, *77*, 255–263; C. A. Naleway, L. A. Curtiss, J. R. Miller, *J. Phys. Chem.* **1991**, *95*, 8434–8437.
- [7] a) A. Harriman, J.-P. Sauvage, *Chem. Soc. Rev.* **1996**, *25*, 41–48; b) M. R. Wasielewski, *Chem. Rev.* **1992**, *92*, 435–461; c) D. Gust, T. A. Moore, A. L. Moore, *Acc. Chem. Res.* **2001**, *34*, 40–48; d) M. N. Paddon-Row, *Adv. Phys. Org. Chem.* **2003**, *38*, 1–85; e) D. Kim, A. Osuka, *Acc. Chem. Res.* **2004**, *37*, 735–745; f) J. L. Sessler, M. Sathiosatham, C. T. Brown, T. A. Rhodes, G. Wiederrecht, *J. Am. Chem. Soc.* **2001**, *123*, 3655–3660.
- [8] a) X. D. Cui, A. Primak, X. Zarate, J. Tomfohr, O. F. Sankey, A. L. Moore, T. A. Moore, D. Gust, G. Harris, S. M. Lindsay, *Science* **2001**, *294*, 571–574; b) J. Reichert, R. Ochs, D. Beckmann, H. B. Webber, M. Mayor, H. van Löhnens, *Phys. Rev. Lett.* **2002**, *88*, 176804(1)–176804(4); c) T. Dadoosh, Y. Gordin, R. Krahn, I. Khivrich, D. Mahalu, V. Frydman, J. Sperling, A. Yacoby, I. Bar-Joseph, *Nature* **2005**, *436*, 677–680; d) L. Venkataraman, J. E. Klare, I. W. Tam, C. Nuckolls, M. S. Hybertsen, M. L. Steigerwald, *Nano Lett.* **2006**, *6*, 458–462; N. Tao, *J. Mater. Chem.* **2005**, *15*, 3260–3263.
- [9] L. Venkataraman, J. E. Klare, C. Nuckolls, M. S. Hybertsen, M. L. Steigerwald, *Nature* **2006**, *442*, 904–907.
- [10] a) A. Helms, D. Heiler, G. McLendon, *J. Am. Chem. Soc.* **1991**, *113*, 4325–4327; b) L. R. Khundkar, J. W. Perry, J. E. Hanson, P. B. Dervan, *J. Am. Chem. Soc.* **1994**, *116*, 9700–9709; c) J. Daub, R. Engl, J. Kurzawa, S. E. Miller, S. Schneider, A. Stockman, M. R. Wasielewski, *J. Phys. Chem. A* **2001**, *105*, 5655–5665; d) B. D. Allen, A. C. Benniston, A. Harriman, L. J. Mallon, C. Pariani, *Phys. Chem. Chem. Phys.* **2006**, *8*, 4112–4118.
- [11] H. J. Van Ramesdonk, B. H. Bakker, M. M. Groeneveld, J. W. Verhoeven, B. D. Allen, J. P. Rostron, A. Harriman, *J. Phys. Chem. A* **2006**, *110*, 13145–13150.
- [12] X. F. Guo, Z. H. Gan, H. X. Luo, Y. Araki, D. Q. Zhang, D. B. Zhu, O. Ito, *J. Phys. Chem. A* **2003**, *107*, 9747–9753.
- [13] I. V. Rubtsov, N. P. Redmore, R. M. Hochstrasser, M. J. Therien, *J. Am. Chem. Soc.* **2004**, *126*, 2684–2685.
- [14] A. C. Benniston, A. Harriman, P. Y. Li, P. V. Patel, C. A. Sams, *J. Org. Chem.* **2006**, *71*, 3484–3493.
- [15] A. C. Benniston, A. Harriman, P. Y. Li, P. V. Patel, C. A. Sams, *Phys. Chem. Chem. Phys.* **2005**, *7*, 3677–3679.
- [16] A. C. Benniston, A. Harriman, P. Y. Li, C. A. Sams, *J. Am. Chem. Soc.* **2005**, *127*, 2553–2564.
- [17] A. C. Benniston, A. Harriman, P. Y. Li, P. V. Patel, J. P. Rostron, C. A. Sams, *J. Phys. Chem. A* **2006**, *110*, 9880–9886.
- [18] A. C. Benniston, A. Harriman, P. V. Patel, C. A. Sams, *Eur. J. Org. Chem.* **2005**, 4680–4686.
- [19] a) A. C. Benniston, G. M. Chapman, A. Harriman, C. A. Sams, *Inorg. Chim. Acta* **2006**, *359*, 753–758; b) A. Harriman, A. Mayeux, C. Stroh, R. Ziessel, *Dalton Trans.* **2005**, 2925–2932; c) A. C. Benniston, G. M. Chapman, A. Harriman, M. Mehrabi, C. A. Sams, *Inorg. Chem.* **2004**, *43*, 4227–4233; d) A. Amini, A. Harriman, A. Mayeux, *Phys. Chem. Chem. Phys.* **2004**, *6*, 1157–1164; e) A. C. Benniston, V. Grosshenny, A. Harriman, R. Ziessel, *Dalton Trans.* **2004**, 1227–1232.
- [20] A. C. Benniston, A. Harriman, P. Y. Li, C. A. Sams, *J. Phys. Chem. A* **2005**, *109*, 2302–2309.
- [21] A. Harriman, S. A. Rostron, A. Khatyr, R. Ziessel, *Discuss. Faraday* **2006**, *131*, 377–391.
- [22] a) M. E. Sigman, G. L. Closs, *J. Phys. Chem.* **1991**, *95*, 5012–5017; b) G. L. Closs, M. D. Johnson, J. R. Miller, P. Piotrowiak, *J. Am. Chem. Soc.* **1989**, *111*, 3751–3753.
- [23] a) R. A. Marcus, *J. Chem. Phys.* **1956**, *24*, 966–978; b) R. A. Marcus, *J. Chem. Phys.* **1956**, *24*, 979–989; c) R. A. Marcus, *J. Chem. Phys.* **1957**, *26*, 867–871.
- [24] H. Sumi, R. A. Marcus, *J. Chem. Phys.* **1986**, *84*, 4894–4914.
- [25] B. D. Allen, A. C. Benniston, A. Harriman, I. Llarena, C. A. Sams, *J. Phys. Chem. A* **2007**, *111*, 2461–2469.
- [26] A. C. Benniston, A. Harriman, P. Y. Li, C. A. Sams, M. D. Ward, *J. Am. Chem. Soc.* **2004**, *126*, 13630–13631.
- [27] We were unable to detect phosphorescence from the free ligands in a glassy matrix at 77 K, even in the presence of 10% iodoethane.
- [28] a) A. Harriman, G. Izzet, *Phys. Chem. Chem. Phys.* **2007**, *9*, 944–948; b) E. M. Kober, T. J. Meyer, *Inorg. Chem.* **1984**, *23*, 3877–3886; c) R. S. Lumpkin, E. M. Kober, L. A. Worl, Z. Murtaza, T. J. Meyer, *J. Phys. Chem.* **1990**, *94*, 239–243.
- [29] a) M. U. Winters, K. Pettersson, J. Martensson, B. Albinsson, *Chem. Eur. J.* **2005**, *11*, 562–573; b) K. Pettersson, J. Wiberg, T. Ljungdahl, J. Martensson, B. Albinsson, *J. Phys. Chem. A* **2006**, *110*, 319–326; c) M. P. Eng, B. Albinsson, *Angew. Chem.* **2006**, *118*, 5754–5757; *Angew. Chem. Int. Ed.* **2006**, *45*, 5626–5629.
- [30] a) M. Sykora, J. R. Kincaid, *Inorg. Chem.* **1995**, *34*, 5852–5856; b) K. Maruszewski, J. R. Kincaid, *Inorg. Chem.* **1995**, *34*, 2002–2006; c) Y. X. Wang, W. Perez, G. Y. Zheng, D. P. Rillema, *Inorg. Chem.* **1998**, *37*, 2051–2059; d) A. A. Bhuiyan, J. R. Kincaid, *Inorg. Chem.* **1998**, *37*, 2525–2530.
- [31] G. L. J. A. Rikken, J. Fölling, P. Wyder, *Phys. Rev. Lett.* **2001**, *87*, 236602(1)–236602(4).

Received: October 2, 2007
Published online: January 18, 2008